Biochemical Pharmacology 118 (2016) 18–30

Contents lists available at ScienceDirect

Biochemical Pharmacology

journal homepage: www.elsevier.com/locate/biochempharm

Chemotherapy enhances tumor vascularization *via* Notch signaling-mediated formation of tumor-derived endothelium in breast cancer

Peng Zhang [a,b,1], Dongxu He [c,1], Zhen Chen [a,1], Qiongxi Pan [a], Fangfang Du [a], Xian Zang [a], Yan Wang [b], Chunlei Tang [a], Hong Li [d], He Lu [e], Xiaoqiang Yao [b], Jian Jin [a,*], Xin Ma [a,b,1,*]

[a] School of Pharmaceutical Sciences, Jiangnan University, Wuxi, China
[b] School of Biomedical Sciences, The Chinese University of Hong Kong, Shatin, New Territories, Hong Kong, China
[c] National Engineering Laboratory for Cereal Fermentation Technology, Jiangnan University, Wuxi, China
[d] DIFEMA, Merci (EA 3829), Faculté de Médecine et de Pharmacie, Université de Rouen, F-76183 Rouen, France
[e] INSERM, UMR-S1165, Hôpital Saint Louis, IUH, Université Paris Diderot, F-75010 Paris, France

ARTICLE INFO

Article history:
Received 3 May 2016
Accepted 8 August 2016
Available online 9 August 2016

Keywords:
Chemotherapy
Breast cancer cells
Endothelial cells
Notch signaling

ABSTRACT

It is believed that tumor cells can give rise to endothelial cells and tumor endothelium has a neoplastic origin. Yet, the stimuli and underlying mechanism remain unclear. Here, we demonstrate that adriamycin or paclitaxel, first-line chemotherapy agent, induced breast cancer cells to generate morphological, phenotypical and functional features of endothelial cells in vitro. In xenografts models, challenges from adriamycin or paclitaxel induced cancer cells to generate the majority of microvessels. Importantly, in breast cancer specimens from patients with neoadjuvant anthracycline-based or taxane-based chemotherapy, tumor-derived endothelial microvessels, lined by EGFR-amplified or/and $TP53^{+}$-$CD31^{+}$ endothelial cells, was significantly higher in patients with progressive or stable disease (PD/SD) than in those with a partial or complete response (PR/CR). Further, exposure to the Notch signaling inhibitor and gene silencing studies showed that Notch signaling inhibition or silencing Nothc4/Dll3 decreased endothelial markers and function of tumor-derived endothelial cells under chemotherapy treatment, which may be through VEGFR3. Thus, our findings demonstrate that chemotherapy induces functional tumor-derived endothelial microvessels by mediating Notch signaling and VEGF signaling, and may provide new targets for anti-angiogenesis therapy in breast cancer.

1. Introduction

Angiogenesis is essential for tumor growth and metastasis. The growth of solid tumors is strictly dependent on the development of an adequate blood supply through neoangiogenesis [1,2]. There are several known modes of blood-vessel formation in normal tissues. Vessel formation can occur by sprouting angiogenesis, by the recruitment of bone-marrow-derived and/or vascular-wall-resident endothelial progenitor cells that differentiate into endothelial cells (ECs), or by a process of vessel splitting known as intussusception. Tumor vasculature is different from that in normal tissues. Unlike normal tissues, which use sprouting angiogenesis, vasculogenesis, and intussusception, tumors not only use all the above modes of vessel formation [3], but also co-opt preexisting vessels, or tumor vessels can be lined by tumor cells (vascular mimicry) or ECs with cytogenetic abnormalities in their chromosomes, derived from putative cancer stem cells.

Numerous studies have demonstrated that the degree of tumor angiogenesis has prognostic impact in different malignancies [4]. In breast cancer, high tumor vascularity is correlated with poor outcome. Conversely, excellent survival has been found in a subset of patients who have tumors with low vascular density [4]. However, while traditional anti-angiogenesis strategies attempt to reduce the tumor vascular supply, their success is restricted by insufficient efficacy or the development of resistance. A phase III clinical trial in patients with advanced-stage triple-negative breast cancer indicated that the addition of bevacizumab, a neutralizing antibody to VEGF-A, to chemotherapy during adjuvant therapy did not improve invasive disease-free survival for patients with triple-negative breast cancer [5]. The mechanisms proposed to explain the resistance to anti-VEGF therapy have focused on the modes of tumor-vessel formation [6–8].

* Corresponding authors at: School of Pharmaceutical Sciences, Jiangnan University, 1800 Lihu Rd, Wuxi, China.
E-mail addresses: jinjian31@126.com (J. Jin), maxin@jiangnan.edu.cn (X. Ma).
[1] These authors contributed equally to this work.

http://dx.doi.org/10.1016/j.bcp.2016.08.008
0006-2952/

Recently, the possibility of tumor cell transdifferentiation into ECs has been suggested in lymphoma [9], myeloma [10], chronic myeloid leukemia [11], and neuroblastoma [12–15]. In breast cancer, the known differentiation potential of cancer stem cells is not only toward the breast glandular epithelial lineages [16,17], but also endothelial cross-lineages [18,19]. However, the impact of chemotherapy on tumor-derived endothelial cells has not yet been explored. In the present study, we demonstrated that breast cancer cells in the context of chemotherapy are able to induce functional tumor-derived endothelial microvessels in clinical samples from neoadjuvant chemotherapy of breast cancer and in vitro/in vivo breast cancer drug resistance cell lines, which is mediated by Notch signaling.

2. Materials and methods

2.1. Ethics statement

All animal experiments were performed in accordance with the laboratory animal guidelines and with approval from the Animal Experimentations Ethics Committee, Jiangnan University. The study using clinical samples was approved by Institutional Review Board at the affiliated hospital, Jiangnan University.

2.2. Patients

Patients were recruited between 2011 and 2013. The protocol included 1–6 cycles of anthracycline-taxane-based chemotherapy for all patients. Tumor assessment was performed by MRI and/or ultrasound depending on those used at baseline. Treatment response was assessed by the RECIST criteria [20]. Patients achieving complete (CR) or partial (PR) response were considered as responder; stable disease (SD) or progressive disease (PD) considered as non-responder.

2.3. Cell culture

MCF-7/WT (ATCC), adriamycin-resistant human breast cancer cells (MCF-7/ADM) or paclitaxel-resistant human breast cancer cells (MCF-7/PTX), GFP stable-labeled MCF-7/ADM (GFP-MCF-7/ADM) and GFP stable-labeled MCF-7/ADM (GFP-MCF-7/PTX) were cultured in RPMI supplemented with 10% FBS, 100 μg/ml penicillin and 100 U/ml streptomycin. MCF-7/ADM or MCF-7/PTX cells were derived by treating MCF-7 cells with stepwise increasing concentration of adriamycin or paclitaxel over 8 months.

2.4. Combined fluorescence in situ hybridization (FISH) and immunofluorescence analysis

FISH was performed using the Vysis EGFR/CEP 7 FISH Probe Kit (LSI EGFR SpectrumOrange/CEP 7 SpectrumGreen probe). Briefly, the sections were deparaffinized, dehydrated in 100% ethanol and dried. Slides were then subjected to protease digestion for 20 min and dehydrated in an ethanol series. The probe set was applied to the selected area on each slide, and the hybridization area was covered with a glass coverslip and sealed with rubber cement. The slides were incubated at 76 °C for 5 min for codenaturation of chromosomal and probe DNA, and hybridization occurred at 37 °C for 16 h in a StatSpin ThermoBrite Slide Hybridizer. After hybridization, the rubber cement was removed and the slides were washed, At this point, slides were processed for immunofluorescence detection of CD31 protein. Slides were incubated for 2 h at 37 °C with the anti-human CD31 (ab9498). After a brief wash, immunodetection was performed using a Alexa Fluor 647 Donkey anti-Mouse IgG Antibody (Life Technologies) for 60 min at room temperature, washed three times in PBS buffer for 5 min. each, and the slides were mounted in antifade solution with DAPI.

2.5. Endothelial function assays

For tube formation assay, basement membrane-like extract (BD/Matrigel) was thawed at 4 °C overnight. 24-well tissue culture plates were coated with 200 μl matrigel and incubated for 30 min at 37 °C to allow the matrix solution to solidify. A total of 2.5×10^5 cells were seeded per well. Cells were inspected under an inverted light microscope. Four representative fields were taken, and the average of the total area of complete tubes formed by the cells was compared using GraphPad Prism computer software. To determine the uptake of acetylated LDLs, cells were incubated with 10 μg/mL Low Density Lipoprotein from Human Plasma, Acetylated, DiI complex (DiI AcLDL) (Invitrogen; L3484) at 37 °C for 4 h. The slides were analyzed using a FV1000 Fluoview confocal system.

2.6. Immunofluorescence analysis

IF staining was performed as previously described [21]. Briefly, cultured cells or frozen sections of xenografts, or surgical specimens were fixed with 4% paraformaldehyde (PFA, Sigma-Aldrich) for 15 min then blocked with 10% BSA with 0.1% Triton X-100 (Bio-Rad) in PBS for 30 min at room temperature. Samples were incubated with primary antibodies overnight at 4 °C followed by the appropriate secondary fluorescently labeled antibodies (Invitrogen Molecular Probes) for one hour at room temperature. Nuclei were counterstained with DAPI. Images were taken with a Leica TCS SP8 confocal microscope. Specific antibodies against CD31 (ab76533; 1:200) or CD146 (AF932; R&D systems; 1:200), vWF (PL030586R; PL laboratories;1:200), E-cadherin (MAB1838; R&D; 1:200), N-cadherin (TA503775S; origene; 1:200), fibronectin (TA505462S; origene; 1:200), vimentin (ab92547;1:200), and eNOS (ab5589; 1:100) were used for the IF staining analysis in cultured cells. Specific antibodies against CD31 (ab7388; 1:10), CD44 (ab6124; 1:100), vimentin (ab92547;1:200); CD31 (ab9498; 1:50) were used for the IF staining analysis in frozen sections of xenografts, or surgical specimens. Secondary antibodies Alexa Fluor 647 Donkey Anti-Rabbit IgG (H+L) antibody, Alexa Fluor 647 Donkey Anti-Mouse IgG (H+L) antibody, Alexa Fluor 568 Donkey anti-Rabbit IgG (H+L) Antibody, Alexa Fluor 488 Donkey Anti-Mouse IgG (H+L) Antibody, Alexa Fluor 568 Donkey Anti-Mouse IgG (H+L) Antibody, Alexa Fluor 488 Donkey Anti-Rabbit IgG (H+L) Antibody were from Invitrogen.

2.7. Immunohistochemistry staining

Tissue slides were deparaffinized with xylene and rehydrated through a graded alcohol series. The endogenous peroxidase activity was blocked by incubation in a 3% (vol/vol) hydrogen peroxide solution for 10 min. Antigen retrieval was carried out by immersing the slides in 10 mM sodium citrate buffer (pH 6.0) and maintaining them at a subboiling temperature for 10 min. The slides were incubated with the primary antibody in 10% (wt/vol) BSA and 0.4% sodium azide in PBS] at 4 °C in a humidified chamber. Subsequently, the sections were incubated with the GTVision III Detection System/Mo&Rb Kit (Gene Tech Company Limited). All staining was assessed by pathologists blinded to the origination of the samples and subject outcome. The widely accepted German semiquantitative scoring system for considering the staining intensity and area extent was used. Each specimen was assigned a score according to the intensity of the membrane (for DLL3) or nuclear (for Notch4) staining (0, no staining; 1, weak staining; 2, moderate staining; 3,

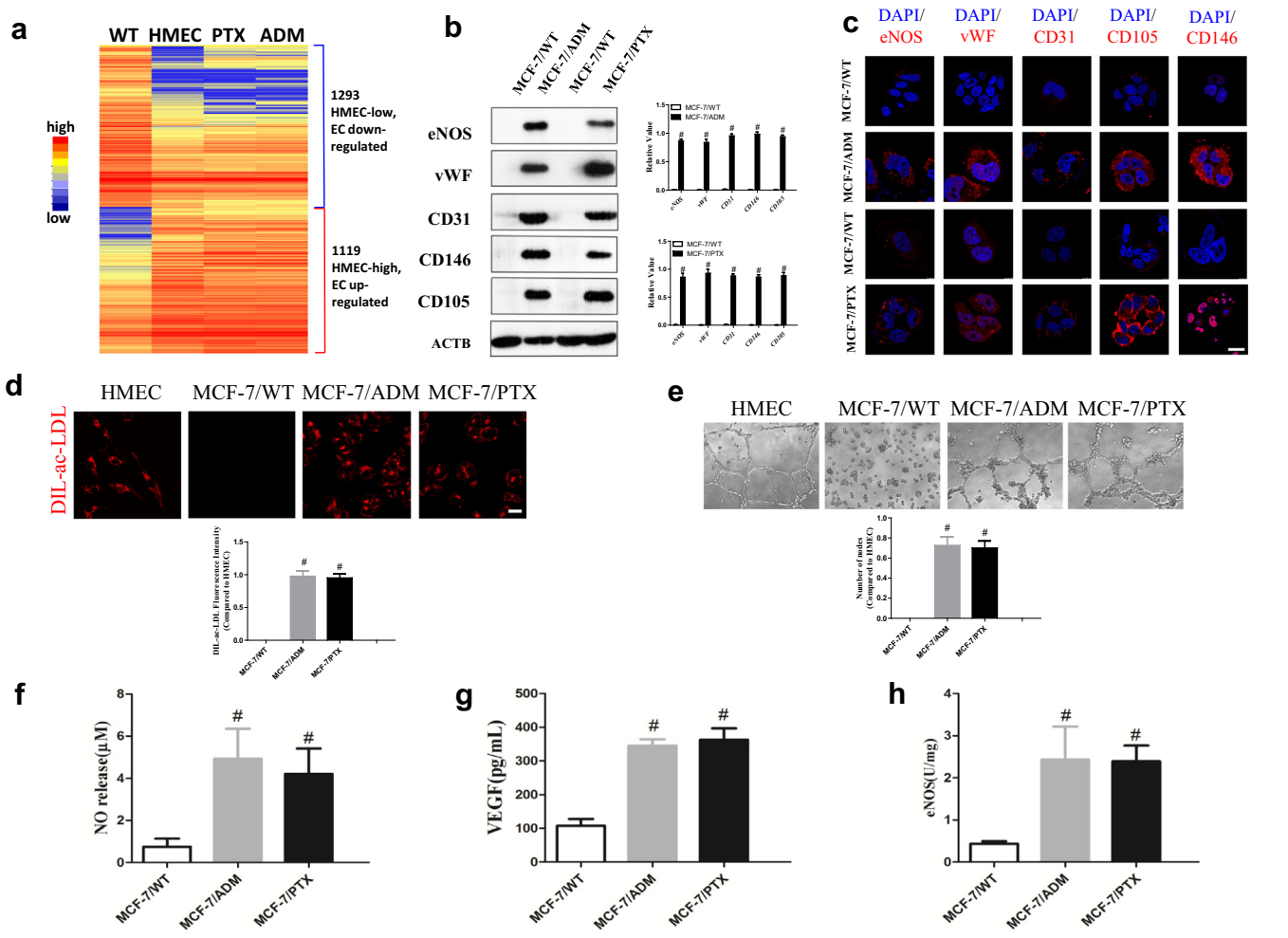

Fig. 1. Adriamycin and paclitaxel induce breast cancer cells to give rise to endothelial cells. (a) RNA expression profiling of MCF7/ADM, PTX, WT and HMEC were analyzed by Illumina Hiseq 2500 system, and gene expression value were shown as FPKM. Significantly changed genes (FDR ⩽ 0.001 and log2Ratio ⩾ 1) between the four cell lines were chosen and hierarchical clustering was performed between the cell lines. (b) Western blotting of CD31, vWF, eNOS, CD105, CD146 and ACTB expression in MCF-7/WT, MCF-7/ADM and MCF-7/PTX cells. (c) Endothelial morphology with EC markers CD31, vWF, eNOS, CD105, and CD146 assessed by immunofluorescence in MCF-7/WT, MCF-7/ADM and MCF-7/PTX cells. Scale bars, 100 μm. (d–f) eNOS expression, VEGF release and NO release assessed by NO kit. (g) Identification of endothelial phenotype by Dil-AcLDL labeling in HMEC, MCF-7/WT, MCF-7/ADM and MCF-7/PTX cells. Scale bars, 100 μm. (h) Tube formation in HMEC, MCF-7/WT, MCF-7/ADM and MCF-7/PTX cells (100×). HMEC, human microvascular endothelial cells. Values are means ± SEM of three to seven experiments. #, $p < 0.05$, compared to MCF-7/WT.

strong staining) and the extent of stained cells (0, 0%; 1, 1–24%; 2, 25–49%; 3, 50–74%; 4, 75–100%). The final immunoreactive score was determined by multiplying the intensity score with the extent of score of stained cells, ranging from 0 (the minimum score) to 12 (the maximum score). For Notch4 and DLL3, we defined 0 score as negative and 1–12 scores as positive, respectively.

2.8. Flow cytometry

Flow cytometry (FACS) was employed to detect CD24 and CD44 on the surfaces of the cells and was carried out with those that have acquired such expression upon transfer of MVs. The cells were detached using trypsin to obtain a single-cell suspension the aliquots of which (1×10^6/samples) were washed in PBS with 1% FBS. The cells then were then stained for 45 min at 4 °C with antibody against CD24 (5 μg/mL) and CD44 (5 μg/mL), washed with PBS and analyzed. The data were acquired using FACScalibur flow cytometer (BD Biosciences, Mountain View, CA) [22].

2.9. Mammosphere assays

Single cells were seeded in ultra-low attachment plates (Corning) at 500 cells/cm^2 in serum-free DMEM/F12 medium (Invitrogen) supplemented with B27 (Invitrogen), 20 ng/mL EGF and 10 ng/mL bFGF (Peprotech). After 6–9 days, count the number of mammospheres which are greater than 50 μm diameter using an inverted light microscope.

2.10. Assay of NO release, eNOS expression and VEGF secretion

The NO release (A012, Nanjing Jiancheng Bioengineering Institute), eNOS activity (H195, Nanjing Jiancheng Bioengineering Institute) and VEGF secretion (Quantikine, R&D Systems) in supernatants were assayed according to the protocols prepared by the manufacturer.

2.11. In vivo tumorigenicity assay

MCF-7/WT, MCF-7/ADM, GFP-MCF-7/ADM, MCF-7/PTX, or GFP-MCF-7/PTX cells were subcutaneously injected into the flanks of female nude mice (5×10^6 cells per mouse) and allowed to propagate for 4–8 weeks with or without estrogen supplementation. All mice were housed in an air-filtered pathogen-free condition. Animals were also injected once every 3 d at the tumor sites with DAPT (75 μM) or 0.1% DMSO for control or DLL3/Notch4-siRNA (40 pmol) or scrambled siRNA as control.

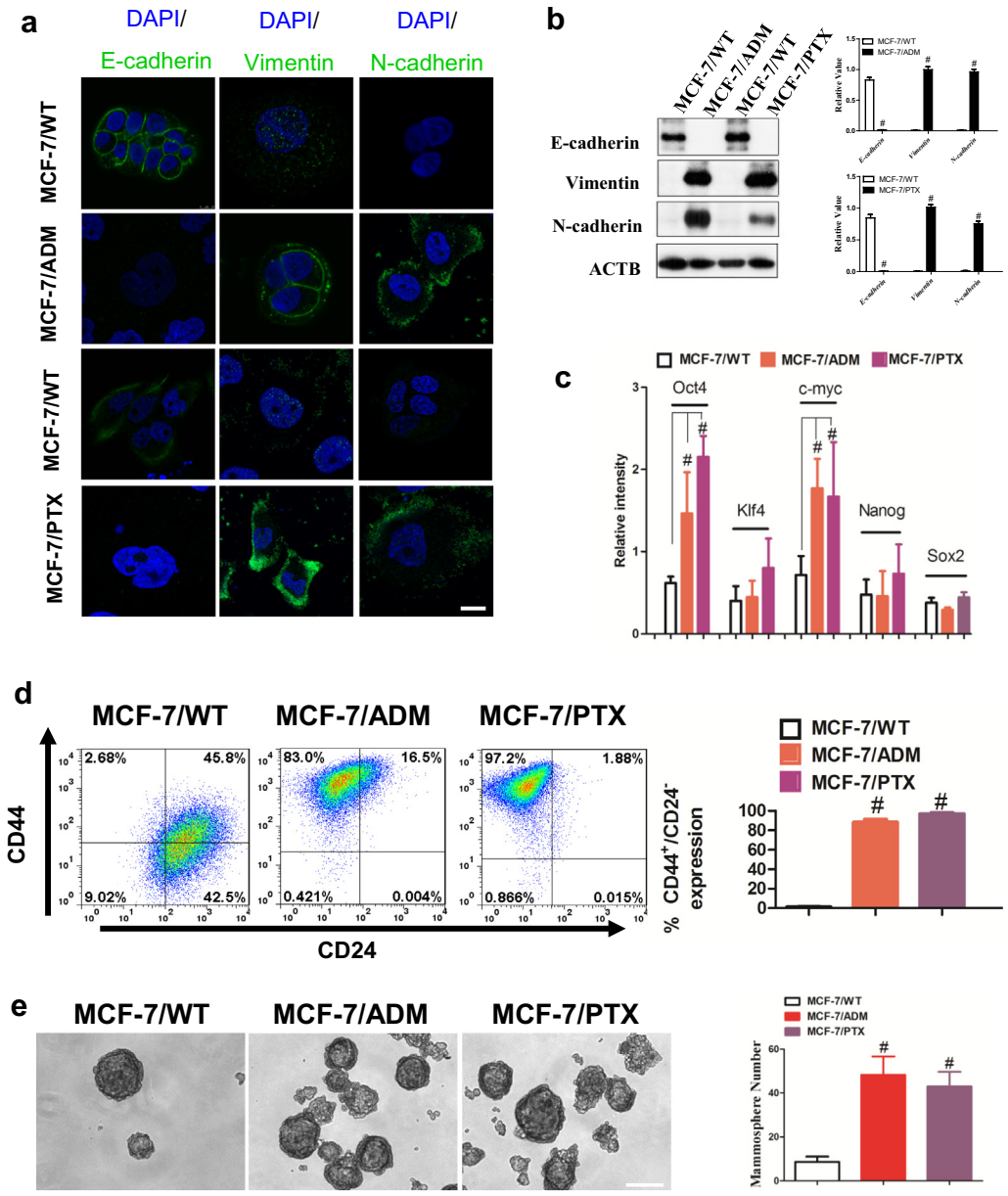

Fig. 2. The endothelial phenotype is associated with EMT/CSC features. (a) Immunofluorescence of EMT markers, E-cadherin vimentin, and N-cadherin in MCF-7/WT, MCF-7/ADM and MCF-7/PTX cells. Scale bars, 100 μm. (b) Western blotting of E-cadherin vimentin, N-cadherin and ACTB expression in MCF-7/WT, MCF-7/ADM and MCF-7/PTX cells. (c) Expression of five transcription factors shown by RT-PCR. (d) CD44/CD24 expression assessed by flow cytometry. Values are means ± SEM of three to eight experiments. Nuclei are stained with DAPI (blue). #, $p < 0.05$, compared to MCF-7/WT. (For interpretation of the references to colour in this figure legend, the reader is referred to the web version of this article.)

2.12. Microvessel staining

Xenografts were harvested immediately for frozen section. Sections were incubated with anti-CD31 antibodies at 4 °C overnight and then secondary antibody for 1 h. Microvessel density was determined by confocal microscopy in areas containing the highest numbers of capillaries and small venules (microvessels). Any endothelial cells or endothelial cell cluster positive for CD31-related antigen and clearly separate from an adjacent cluster was considered to be a single, countable microvessel. Results were expressed as the highest number of microvessels identified within any single 200 × field [4].

2.13. RT-PCR and quantitative real-time PCR

cDNAs from isolated microvesicles were obtained using Reverse Transcriptase M-MLV (RNase H-) kit (TaKaRa). RT-PCR was performed using Thermal Cycler C1000 Tech (Bio-Rad). In peripheral blood from patients, the primer pairs for Oct4 were forward 5′-AGC GAACCAGTATCGAGAAC-3′, reverse 5′-TTACAGAACCACACTCGGAC-3′, Sox2 were forward 5′-AGCTACAGCATGATGCAGGA-3′, reverse 5′-GGTCATGGAGTTGTACTGCA-3′, Klf4 were forward 5′-TCTCAAGGCA CACCTGCGAA-3′, reverse 5′-TAGTGCCTGGTCAGTTCATC-3′, c-myc were forward 5′-ACTCTGAGGAGGAACAAGAA-3′, reverse 5′-TGGA GACGTGGCACCTCTT-3′, nanog were forward 5′-TGAACCTCAGCTA

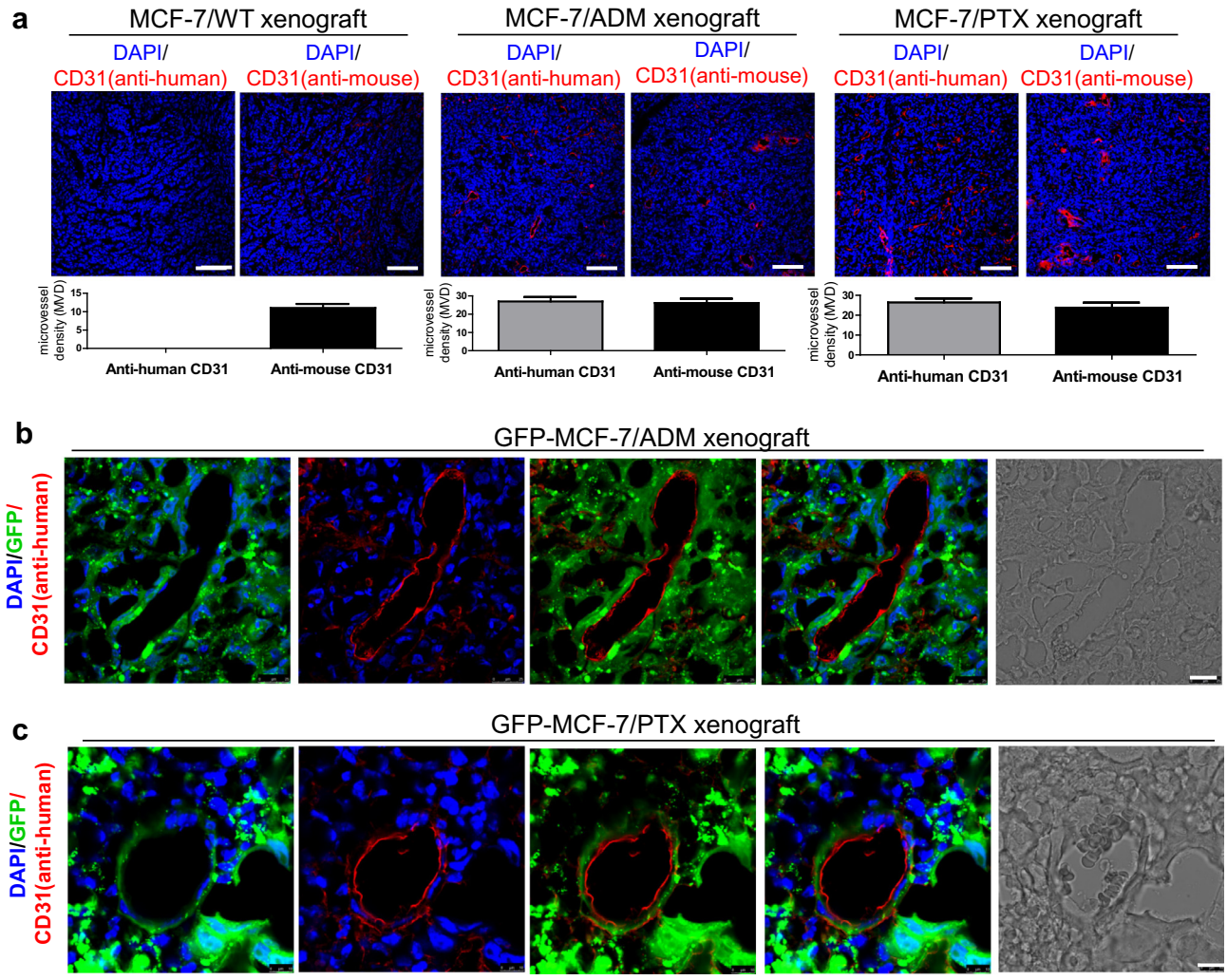

Fig. 3. Adriamycin and paclitaxel induce functional human-derived endothelial microvessels in human breast cancer xenografts (a) Immunofluorescence of tumor-derived endothelial microvessels for CD31 (anti-human) or CD31 (anti-mouse) in MCF-7/WT (left), MCF-7/ADM (middle), and MCF-7/PTX (right) xenografts. Scale bars, 100 μm. (b and c) In vivo lineage tracing of tumor-derived endothelial microvessels in MCF-7/ADM and MCF-7/PTX xenografts with constitutive GFP expression and immunofluorescence of EC marker CD31. Scale bars, 25 μm.

CAAACAG-3′, reverse 5′-TGGTGGTAGGAAGAGTAAAG-3′, Notch4 were forward 5′-CCCAGGAATCTGAGATGGAA-3′, reverse 5′-CCA CAGCAAACTGCTGACAT-3′, actin were forward 5′-TGAAGTGTGAC GTGGACATC-3′, reverse 5′-GGAGGAGCAATGATCTTGAT-3. Quantitative real-time PCR was performed using SYBR Green master mix (Applied Biosystems, Foster City, CA) on 7500 Fast Real-time PCR system (Applied Biosystems). Relative gene expression was normalized against ACTB. Primers were: DLL1 forward 5′-TGCCTG GATGTGATGAGCAGCA-3′, reverse 5′-ACAGCCTGGATAGCGGATA CAC-3′; DLL3 forward 5′-CACTCAACAACCTAAGGACGCAG-3′, reverse 5′-GAGCGTAGATGGAAGGAGCAGA-3′; DLL4 forward 5′-CT GCGAGAAGAAAGTGGACAGG-3′, reverse 5′-ACAGTCGCTGACGTG GAGTTCA-3′; Jagged1 forward 5′-TGCTACAACCGTGCCAGTGACT-3′, reverse 5′-TCAGGTGTGTCGTTGGAAGCCA-3′; Jagged2 forward 5′-GCTGCTACGACCTGGTCAATGA-3′, reverse 5′-AGGTGTAGGCATCG CACTGGAA-3′; Notch1 forward 5′-CCCAGGAATCTGAGATGGAA-3′, reverse 5′-CCACAGCAAACTGCTGACAT-3′; Notch2 forward 5′-GTGC CTATGTCCATCTGGATGG-3′, reverse 5′-AGACACCTGAGTGCTGGCA CAA-3′; Notch3 forward 5′-TACTGGTAGCCACTGTGAGCAG-3′, reverse 5′-CAGTTATCACCATTGTAGCCAGG-3′.

HeyL forward 5′-TGGAGAAAGCCGAGGTCTTGCA-3′, reverse 5′-ACCTGATGACCTCAGTGAGGCA-3′; SNAI1 forward 5′-TGCCCTCA AGATGCACATCCGA-3′, reverse 5′-GGGACAGGAGAAGGGCTTCTC-3′; SNAI2 forward 5′-ATCTGCGGCAAGGCGTTTTCCA-3′, reverse 5′-GA GCCCTCAGATTTGACCTGTC-3′; VEGFR3 forward 5′-TGCGAA TACCTGTCCTACGATGC-3′, reverse 5′-CTTGTGGATGCCGAAAGCG GAG-3′; ACTB forward 5′-CACCATTGGCAATGAGCGGTTC-3′, reverse 5′-AGGTCTTTGCGGATGTCCACGT-3′.

2.14. Gene array

Total RNA was extracted from MCF-7/WT, MCF-7/ADM and MCF-7/PTX. Gene array was performed by BGI company.

2.15. Western blot analysis

Cells were lysed using a detergent extraction buffer containing 1% (vol/vol) Nonidet P-40, 150 mmol/L NaCl, and 20 mmol/L Tris–HCl, pH 8.0, with the addition of protease inhibitor cocktail tablets and centrifuged for 15 min at 4 °C. Protein concentrations were then measured using a Bio-Rad protein assay kit (Hercules, California). Proteins were separated on an 8%–12% gel using sodium dodecyl sulfate polyacrylamide gel electrophoresis. For immunoblots, the polyvinylidene difluoride membrane carrying the trans-

Table 1
Clinical and pathological characteristics of 40 breast cancer patients enrolled in this study.

	All Patients (n = 40)		PD/SD (n = 18)		PR/CR (n = 22)	
Age(years)						
<50	19(47.5%)		10(55.6%)		8(36.4%)	
⩾50	21(52.5%)		8(44.4%)		14(63.6%)	
Sex						
Male	0(0.0%)		0(0.0%)		0(0.0%)	
Female	40(100.0%)		18(100.0%)		22(100.0%)	
Histology						
Ductal	40(100.0%)		18(100.0%)		22(100.0%)	
Breast cancer	Pre-	Post-	Pre-	Post-	Pre-	Post-
Tumor size						
Tx	0(0.0%)	1(2.5%)	0(0.0%)	0(0.0%)	0(0.0%)	1(4.5%)
T1	4(10.0%)	8(20.0%)	2(11.1%)	2(11.1%)	2(9.1%)	6(27.3%)
T2	17(42.5%)	16(40.0%)	7(38.9%)	8(44.4%)	10(45.5%)	8(36.4%)
T3	12(30.0%)	9(22.5%)	5(27.8%)	3(16.7%)	7(31.8%)	6(27.3%)
T4	7(17.4%)	6(15.0%)	4(22.2%)	5(27.8%)	3(13.6%)	1(4.5%)
Lymph node status						
Nx	6(15.0%)	1(2.5%)	5(27.8%)	0(0.0%)	1(4.5%)	1(4.5%)
N0	10(25.0%)	8(20.0%)	5(27.8%)	4(22.2%)	5(22.7%)	4(18.2%)
N1	12(30.0%)	10(25.0%)	5(27.8%)	4(22.2%)	7(31.9%)	6(27.3%)
N2	6(15.0%)	12(30.0%)	2(11.1%)	6(33.4%)	4(18.2%)	6(27.3%)
N3	6(15.0%)	9(22.5%)	1(5.5%)	4(22.2%)	5(22.7%)	5(22.7%)
AJCC Substage						
I	0(0.0%)	0(0.0%)	0(0.0%)	0(0.0%)	0(0.0%)	0(0.0%)
II	15(37.5%)	16(40.0%)	8(44.4%)	5(27.8%)	7(31.8%)	11(50.0%)
III	17(42.5%)	14(35.0%)	6(33.3%)	7(38.9%)	11(50.0%)	7(31.8%)
IV	8(20.0%)	10(25.0%)	4(22.3%)	6(33.3%)	4(18.2%)	4(18.2%)
Adjuvant chemotherapy						
Anthracycline	5(12.5%)	6(15.0%)	3(16.7%)	3(16.7%)	2(9.1%)	3(13.6%)
Taxane	4(10.0%)	12(30.0%)	0(0.0%)	6(33.3%)	4(18.2%)	6(27.3%)
Anthracycline/Taxane	31(77.5%)	22(55.0%)	15(83.3%)	9(50.0%)	16(72.7%)	13(59.1%)

ferred proteins was incubated at 4 °C overnight with designated primary antibodies diluted (1:1000) in TBST buffer containing 0.1% Tween20 and 5% non-fat dry milk. Immunodetection was accomplished by using a horseradish peroxidase-conjugated secondary antibody (1:3000) and an enhanced chemiluminescence detection system (GE Healthcare). Antibodies Notch1(#3608), Notch2(#5732), Notch3(#5276), Notch4(#2423), DLL1(#2588), DLL4(#2589), Jagged1(#2620), Jagged2(#2210) were from CST; DLL3 (ab103102), p65 (ab16502) from Abcam; ZEB1(sc-25388), Flt4(sc-321)from santa cruz.

2.16. Small interfering RNA (siRNA) transfection

For knockdown of Notch4, DLL3 and VEGFR3 transcripts, MCF-7/ADM and MCF-7/PTX cells were transiently transfected with gene-specific or scrambled small interfering RNA (siRNA) using DharmaFECT 1 Transfection Reagent (GE Healthcare) following the standard procedure recommended by the manufacturer. ON-TARGET plus SMART pool siRNA was obtained from Dharmacon, Inc. In brief, cells were transfected in RPMI 1640 medium with 100 nM of each siRNA duplex using DharmaFECT transfection reagent according to the manufacturer's protocol. After 48 h transfection, total RNA or protein was then isolated respectively.

2.17. Statistical analyses

Results are presented as mean ± SEM. We assessed comparisons between groups by one-way ANOVA test or Student's *t*-test. We performed the statistical analyses using Graphpad Prism 5.0 software. All statistical tests were two-sided, and *P* values <0.05 were considered to be statistically significant.

3. Results

3.1. Adriamycin and paclitaxel, first-line chemotherapy agent, induce breast cancer cells to give rise to endothelial cells

The MCF-7 cell line was chosen to investigate phenotypic changes under chemotherapy because it is an established model of well-differentiated, luminal breast cancer. Neoadjuvant anthracycline-based adriamycin and taxane-based paclitaxel are the most commonly used chemotherapies in breast cancer patients. MCF-7 cells were treated with stepwise increasing concentrations of either adriamycin or paclitaxel over eight months to mimic the clinical cycles of neoadjuvant chemotherapy, then MCF-7/ADM and MCF-7/PTX cells were generated. We first examined the gene-expression signatures enriched by chemotherapy. RNA extracted from the three cell lines and HMECs were quantified using an RNA sequencing-based expression analysis. Interesting, MCF-7/ADM and MCF-7/PTX cells are similar to HMECs with respect to their global transcriptome (Fig. 1a). Further, to expand on this observation, we utilized western blot and immunofluorescence to examine the endothelial markers including CD31, vWF, eNOS, CD105, and CD146 in MCF-7/WT, MCF-7/ADM and MCF-7/PTX cells. We found that MCF-7/WT did not express any of the endothelial markers, but after long-term treatment with adriamycin or paclitaxel, the expression of CD31, vWF, eNOS, CD105, and CD146 were significantly induced in MCF-7/ADM and MCF-7/PTX cells, exhibiting endothelial morphology (Fig. 1b and c). Such MCF-7/ADM and MCF-7/PTX cells showed formation of capillary-like structures in matrigel and low-density lipoprotein (LDL) uptake ability, which were completely absent in MCF-7/WT cells, suggesting an endothelial phenotype (Fig. 1d and e). We also

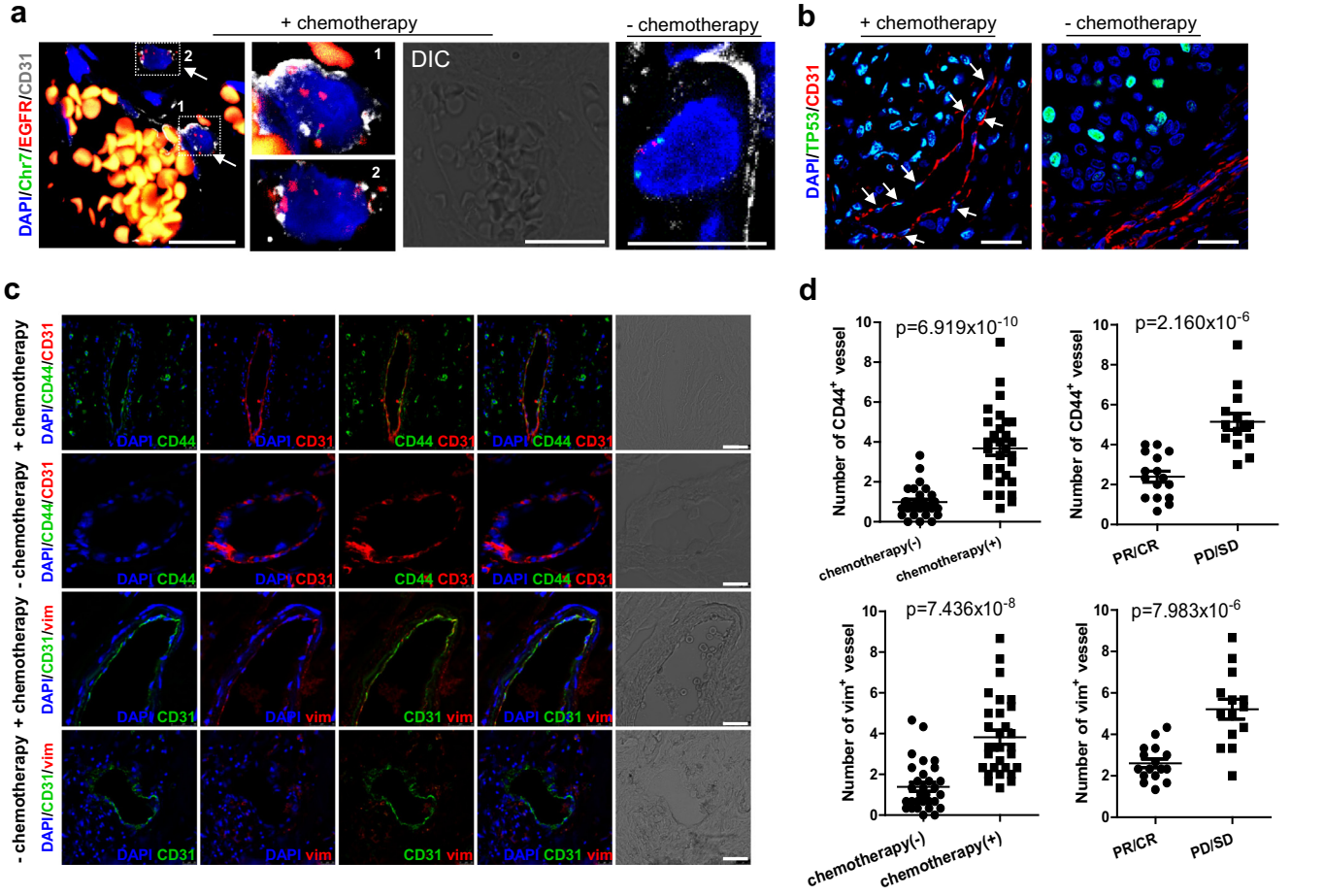

Fig. 4. Chemotherapy induces endothelial cells of tumor origin having EMT/CSC features in breast cancer patients (a) Fluorescence is situ hybridization for epidermal growth factor rector (EGFR, red) and chromosome 7 centromere (Chr7, green) combined with immunofluorescence for CD31 (an EC marker; white). Nuclei are stained with DAPI (blue); erythrocytes are in organge; Arrows indicate $CD31^+$ endothelial microvessel (green) carrying EGFR amplification (multiple red signals) in samples from breast cancer with neoadjuvant chemotherapy. (b) Immunofluorescence of mutant TP53 and CD31 in samples from breast cancer. Arrows indicate $TP53^+$ endothelial microvessel (green) carrying TP53 mutation in samples from breast cancer with neoadjuvant chemotherapy. (c) Representative images and summary data from immunostaining of CD44 (a CSC marker; green) and CD31 (red) in samples from breast cancer. (d) Representative images and summary data from immunostaining of vimentin (a mesenchymal marker; green) and CD31 (red) in samples from breast cancer of human subjects with and without neoadjuvant anthracycline-taxane-based chemotherapy (n = 40). (For interpretation of the references to colour in this figure legend, the reader is referred to the web version of this article.)

assessed the eNOS expression, NO release and VEGF secretion in the three cell lines and found that both MCF-7/ADM and MCF-7/PTX cells had greater eNOS expression, higher NO release and enhanced VEGF secretion than MCF-7/WT cells (Fig. 1f–h). Together, these results suggest that chemotherapy is able to induce breast cancer cells to give rise to functional endothelial cells.

3.2. The endothelial phenotype is associated with EMT/CSC features

We further assessed the expression of several EMT-related genes in MCF-7/WT, MCF-7/ADM and MCF-7/PTX cells by western blot and immunofluorescence. Chemotherapy treatment induced expression of vimentin and N-cadherin, and decreased E-cadherin (Fig. 2a and b). Given the mechanistic link between EMT and CSC phenotypes, we measured the expression of five transcription factors that are characteristic of stem cells, Oct4, Nanog, Klf4, Sox2, and c-myc, as well as the expression of breast cancer stem cell marker $CD44^{high}CD24^{-/low}$. C-myc and Oct4 were consistently and significantly upregulated in MCF-7/ADM and MCF-7/PTX cells (Fig. 2c). Both lines displayed increased CD44 such that the proportion of gated $CD44^{high}CD24^{-/low}$ cells increased ~30-fold in MCF-7/ADM cells and ~36-fold in MCF-7/PTX cells (Fig. 2d). These results indicate that the endothelial phenotype is also associated with EMT/CSC features.

3.3. Adriamycin and paclitaxel induce human-derived functional endothelial microvessels in human breast cancer xenografts

To explore the effect of chemotherapy induced breast cancer cells to form endothelial vessels in vivo, we measured the relative number of human origin endothelial cells within MCF-7/WT, MCF-7/ADM and MCF-7/PTX xenografts. MCF-7/WT cells were additionally inoculated into athymic nude mice with estrogen supplementation. Immunofluorescence of subcutaneous xenografts showed MCF-7/ADM and MCF-7/PTX–derived tumors contained human origin mircovessels marked by anti-human specific CD31 antibody, whereas xenografts generated with MCF-7/WT were almost completely absent of anti-human $CD31^+$ microvessels (Fig. 3a). Moreover, anti-mouse $CD31^+$ vessels were found in all of them (Fig. 3a). To further confirm the presence of human origin endothelial cells in vivo, we investigated the origin of endothelial cells in MCF-7/ADM and MCF-7/PTX xenografts in a lineage-tracing study by transducing MCF-7/ADM and MCF-7/PTX cells with constitutive GFP expression, and implanted the cells to establish xenografts in nude mice (Fig. 3b and c). Tumor samples of the

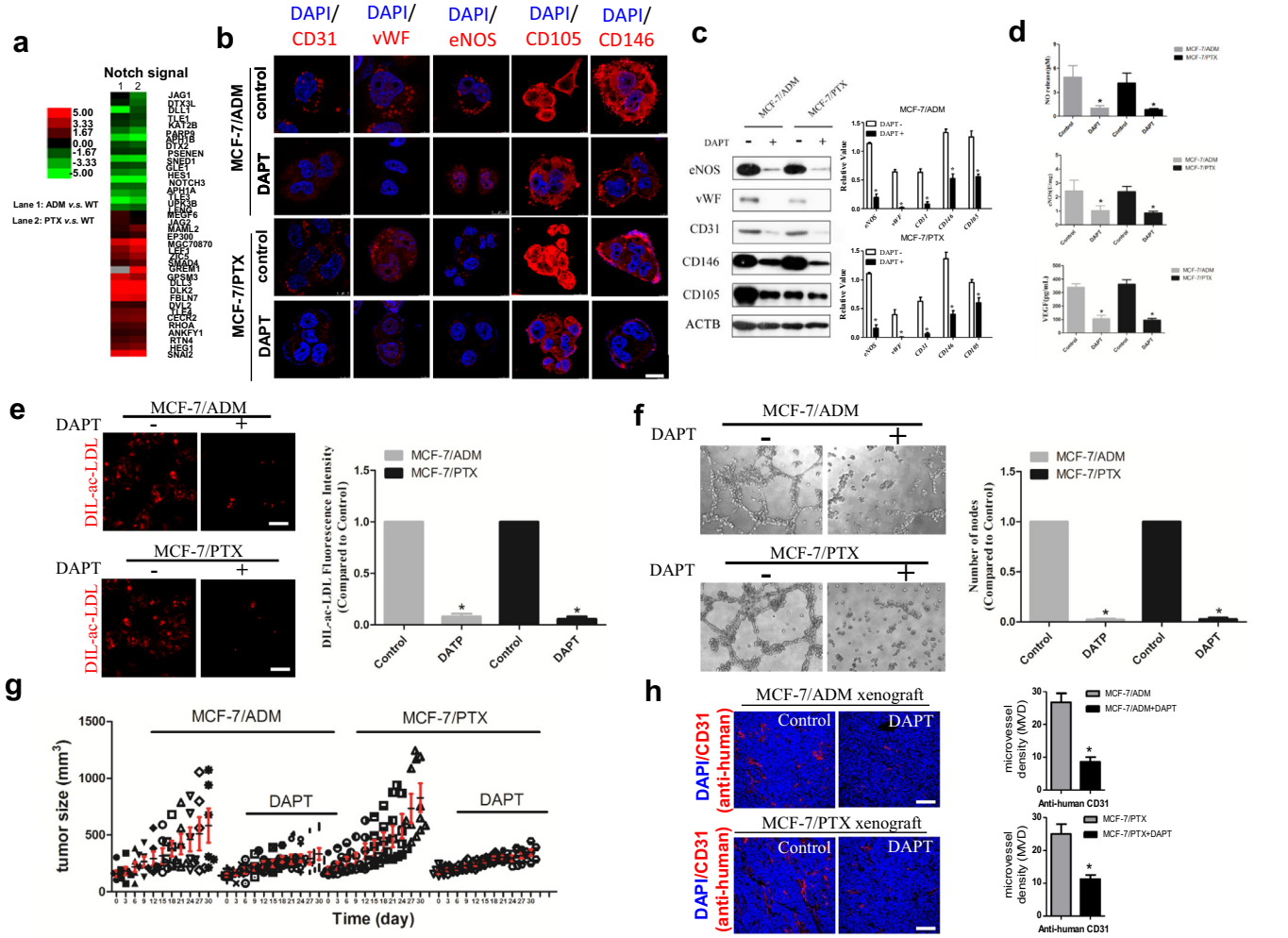

Fig. 5. DAPT blocks the function of tumor-derived of endothelial cells under chemotherapy (a) Average linkage hierarchical clustering according to the full gene expression profiles of MCF-7 cells treated with either adriamycin (MCF-7/ADM) or paclitaxel (MCF-7/PTX). Heatmap of transcripts related to Notch signaling. Intensities are measured in base 2 logarithms ranging from green (down regulation) to red (up regulation). Lane 1, MCF7/ADM *v.s.* MCF-7/WT; Lane 2, MCF7/PTX *v.s.* MCF-7/WT; (b) Endothelial morphology with EC markers CD31, vWF, eNOS, CD105, and CD146 assessed by immunofluorescence in MCF-7/ADM and MCF-7/PTX cells with or without DAPT 75 μM. Scale bars, 100 μm. (c) Western blotting of CD31, vWF, eNOS, CD105, CD146 and ACTB expression in MCF-7/ADM and MCF-7/PTX cells with or without DAPT 75 μM. (d) eNOS expression, VEGF release and NO release assessed by NO kit. (e) Identification of endothelial phenotype by Dil-AcLDL labeling in MCF-7/WT, MCF-7/ADM and MCF-7/PTX cells with or without DAPT 75 μM. Scale bars, 100 μm. (f) Tube formation in MCF-7/ADM and MCF-7/PTX cells with or without DAPT 75 μM (100×). (g) Tumorigenic potential analysis without estrogen supplementation. Female nude mice bearing xenograft tumors derived from MCF-7/ADM or MCF-7/PTX cells were injected at the tumor sites with DAPT (75 μM). (h) Immunofluorescence of tumor-derived endothelial microvessels for CD31 (anti-human) in MCF-7/ADM and MCF-7/PTX xenografts. Quantifications show fractions of tumor-derived endothelial microvessels. Scale bars, 100 μm. Values are means ± SEM of three to eight experiments. *, $p < 0.05$, compared to MCF-7/ADM or MCF-7/PTX. (For interpretation of the references to colour in this figure legend, the reader is referred to the web version of this article.)

xenografts derived from the GFP-labeled cells were immunostained for an endothelial cell marker (CD31, anti-human). Immunofluorescence analyses confirmed that expression of the EC marker overlapped with GFP in the majority of ECs (mean 60%, range 40%–80%), indicating that the most of the vascular ECs were of human origin (Fig. 3b and c). Endothelial microvessels formed by tumor cells displayed an open lumen and consistently contained erythrocytes, indicating that these vessels were functional (Fig. 3b and c). Notably, a minor fraction (mean 30%, range 10%–40%) of vascular ECs in the xenografts did not have GFP expression, indicating that these ECs were derived from the host (Fig. 3b and c).

3.4. Chemotherapy promotes the tumor origin of endothelial cells formation in clinical breast cancer patients

To investigate the clinical relevant of chemotherapy-induced tumor-derived microvessels in breast cancer, we analyzed breast cancer tissue from 40 patients with and without anthracycline-taxane-based chemotherapy (Table 1). Amplification of the epidermal growth factor receptor (EGFR) oncogene and mutation of TP53 were chosen as tumor-specific genetic markers [23]. They are associated with a poor response to chemotherapy and linked to the induction of an epithelial-mesenchymal transition (EMT) and acquisition of stemness properties [24–28]. We performed combined CD31 immunofluorescence and fluorescence in situ hybridization (FISH) analyses for EGFR and chromosome 7, and immunostaining for TP53 mutation and CD31 in 6 breast tumors with and 18 tumors without neoadjuvant chemotherapy. In tumors with neoadjuvant chemotherapy, $CD31^+$ ECs were detected with EGFR signals: cells with multiple red hybridization signals were indicative of EGFR amplification, while cells with two red signals imply single copy of EGFR gene (Fig. 4a). Thus, the former ECs were of tumor origin because they showed the same genetic abnormality as malignant cells, whereas the latter ECs were non-tumor origin. Endothelial microvessels lined by EGFR-amplified $CD31^+$ ECs

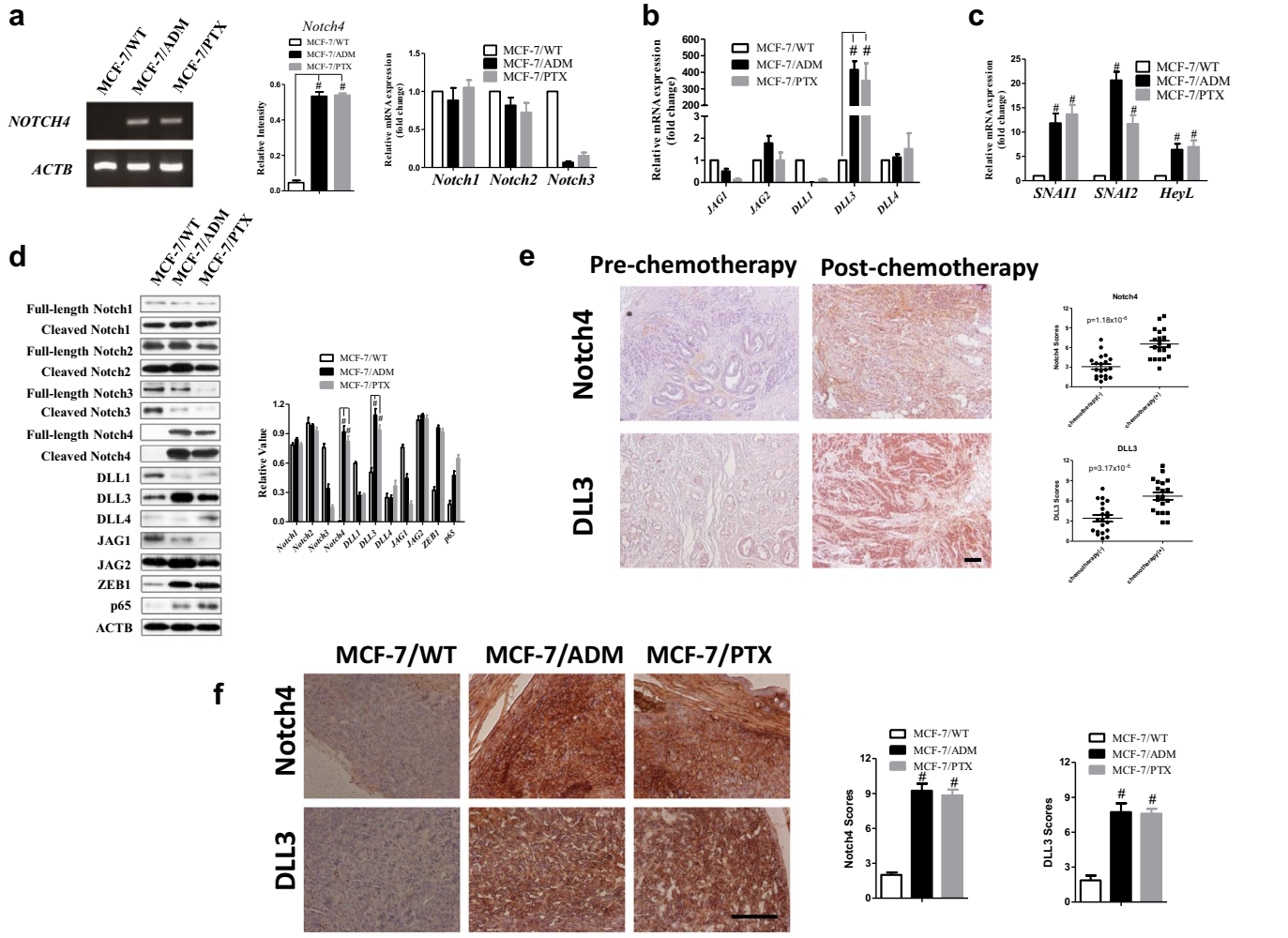

Fig. 6. High-level expression of DLL3 and Notch4 are associated with tumor-derived endothelial cells. (a) RT-PCR for *Notch4* mRNA and Real-time reverse transcription-PCR for *Notch1*, *Notch2* and *Notch3* mRNA in MCF-7/WT, MCF-7/ADM and MCF-7/PTX cells. (b) Real-time reverse transcription-PCR for five Notch ligands mRNA in three cell lines. (c) Real-time reverse transcription-PCR for three Notch targeted genes mRNA in three cell lines. (d) Western blot was used to quantify Notch pathway genes at the protein levels in three cell lines. (e) Representative images and summary data from immunohistochemical staining of Notch4 and DLL3 in paired pre- and post-chemotherapy breast cancer tissue from patients showing elevated Notch4 and DLL3 expression (n = 40). (f) Representative images and summary data from immunohistochemical staining of Notch4 and DLL3 in MCF-7/WT, MCF-7/ADM and MCF-7/PTX xenografts. #, $p < 0.05$, compared to MCF-7/WT.

displayed an open lumen and contained clearly visible erythrocytes (organge). However, EGFR-amplified CD31$^+$ ECs were hardly detected in tumors without neoadjuvant chemotherapy (Fig. 4a). Additionally, CD31$^+$ ECs were detected with TP53 signals and endothelial microvessels lined by TP53$^+$ ECs could be also detected in tumors with chemotherapy, while not in tumors without chemotherapy/Similar results were obtained by TP53 immunofluorescence staining (Fig. 4b).

We also performed immunofluorescence staining of the EC marker CD31 and the mesenchymal marker vimentin, or the CSC marker CD44. We found that in human breast cancer sections, both CD44$^+$- and vimentin$^+$-microvessels were significantly up-regulated after chemotherapy (Fig. 4c and d). Treatment response was assessed by the RECIST criteria. Among 30 patients, 16 patients respond to chemotherapy (PR/CR), while 14 were not responsive (PD/SD). Importantly, both CD44$^+$- and vimentin$^+$-microvessels significantly greater in patients with PD/SD than in those with PR/CR (Fig. 4c and d), indicating its close association with the induction of chemoresistance. Thus, chemotherapy promotes the tumor origin of endothelial cells formation in clinical breast cancer patients.

3.5. Notch signaling regulates function of tumor-derived endothelial cells under chemotherapy treatment

Pathway analysis showed that Notch signaling was enriched both receptors and ligands in MCF-7/ADM and MCF-7/PTX cells by using an RNA sequencing array (Fig. 5a). To confirm Notch pathway is important in the endothelial differentiation of breast cancer cells, we investigated the impact of DAPT, a Notch pathway inhibitor. We found that endothelial markers, CD31, vWF, eNOS, CD105, and CD146, were significantly decreased in MCF-7/ADM and MCF-7/PTX cells after Notch pathway inhibition (Fig. 5b and c). Next we found that eNOS expression, NO release and VEGF secretion were markedly decreased in MCF-7/ADM and MCF-7/PTX cells after DAPT treatment (Fig. 5d). DAPT impaired ability of tube formation in matrigel and low-density lipoprotein (LDL) uptake in MCF-7/ADM and MCF-7/PTX cells (Fig. 5e and f). Further, DAPT treated MCF-7/ADM or MCF-7/PTX xenografts grew slower than those without DAPT treatment (Fig. 5g). We also examined the effect of DAPT on microvessel density by using anti-human specific CD31 antibody. The results showed that tumors with DAPT treatment contained significantly lower microvessel density than those

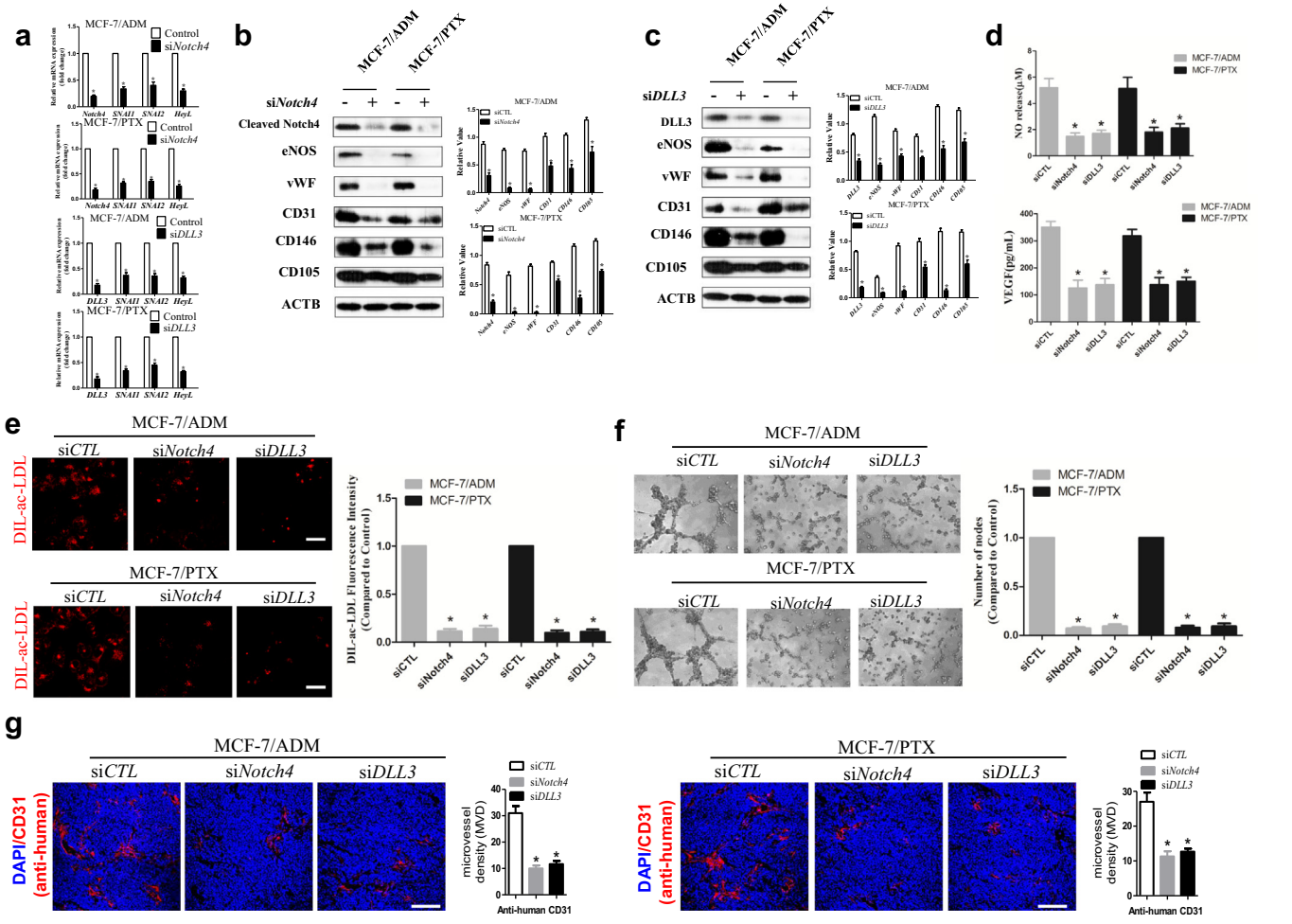

Fig. 7. DLL3 and Notch4 regulate the function of tumor-derived endothelial cells under chemotherapy treatment (a) Real-time reverse transcription-PCR for *Notch4*, *DLL3* and three Notch targeted genes mRNA in MCF-7/ADM and MCF-7/PTX cells transfected with specific siRNA. (b) Western blot for cleaved Notch4, EC markers and ACTB in MCF-7/ADM and MCF-7/PTX cells transfected with specific siRNA. (c) Western blot for DLL3, EC markers and ACTB in MCF-7/ADM and MCF-7/PTX cells transfected with specific siRNA. (d) VEGF release and NO level in MCF-7/ADM and MCF-7/PTX cells transfected with specific siRNA. (e) Identification of endothelial phenotype by Dil-AcLDL labeling in MCF-7/ADM and MCF-7/PTX cells transfected with specific siRNA. Scale bars, 100 μm. (f) Tube formation in MCF-7/ADM and MCF-7/PTX cells transfected with specific siRNA (100×). (g) Immunofluorescence of tumor-derived endothelial microvessels for CD31 (anti-human) in MCF-7/ADM and MCF-7/PTX xenografts. Quantifications show fractions of tumor-derived endothelial microvessels. Scale bars, 100 μm. Values are means ± SEM of three to eight experiments. *, $p < 0.05$, compared to MCF-7/ADM or MCF-7/PTX.

without DAPT treatment (Fig. 5h). Collectively, these data suggest that Notch pathway inhibition resulted in significant function suppression of tumor-derived endothelial cells.

3.6. DLL3 and Notch4 expression are elevated in tumor-derived endothelial cells

To further confirm the mechanism of Notch pathway in tumor-derived endothelial cells during chemotherapy treatment, we first examined the transcriptional alterations of the core Notch pathway genes, including Notch ligands (Jagged-1, Jagged-2, DLL1, DLL3 and DLL4), Notch receptors (Notch1, Notch2, Notch3, Notch4), Notch-targeted genes (SNAI1, SNAI2 and HeyL) in MCF-7/WT, MCF-7/ADM and MCF-7/PTX cells. We found that MCF-7/ADM and MCF-7/PTX cells had greater expression of Notch receptor Notch4 (Fig. 6a) and Notch ligand DLL3 (Fig. 6b) transcripts compared with MCF-7/WT cells. Consistent with Notch pathway activation, striking overexpression of the Notch target genes SNAI1, SNAI2 and HeyL were observed, which are reported to regulate EMT and stemness (Fig. 6c) [29,30]. We also assessed the levels of Notch pathway at protein levels and found that full length/cleaved Notch4 and DLL3 protein expression were significantly increased in MCF-7/ADM and MCF-7/PTX cells (Fig. 6d). In addition, immunohistochemistry showed that both Notch4 and DLL3 expressions were significantly up-regulated in clinical patients with chemotherapy (Fig. 6e). Notch4 and DLL3 expressions were also increased in MCF-7/ADM and MCF-7/PTX xenografts (Fig. 6f). It is reported that the Notch pathway greatly induced expression of several NF-κB subunits [31], which has been identified as a crucial mediator of EMT in cancer progression [32]. It is known that ZEB1 is a transcriptional repressor to the expression of E-cadherin, resulting in the induction of the EMT phenotype [33]. NF-κB could up-regulated ZEB1 expression [31]. Therefore, we assessed whether the expression of Notch downstream target NF-κB subunit p65 and ZEB1 is altered in MCF-7/ADM and MCF-7/PTX cells. We found that p65 and ZEB1were greatly up-regulated (Fig. 6d).

3.7. DLL3 and Notch4 regulate the function of tumor-derived endothelial cells under chemotherapy treatment

To investigate whether DLL3 and Notch4 are important in the tumor-derived endothelial cells, we investigated the impact of gene silencing of Notch4 and DLL3 using specific siRNAs. The results showed that the expressions of Notch target genes SNAI1,

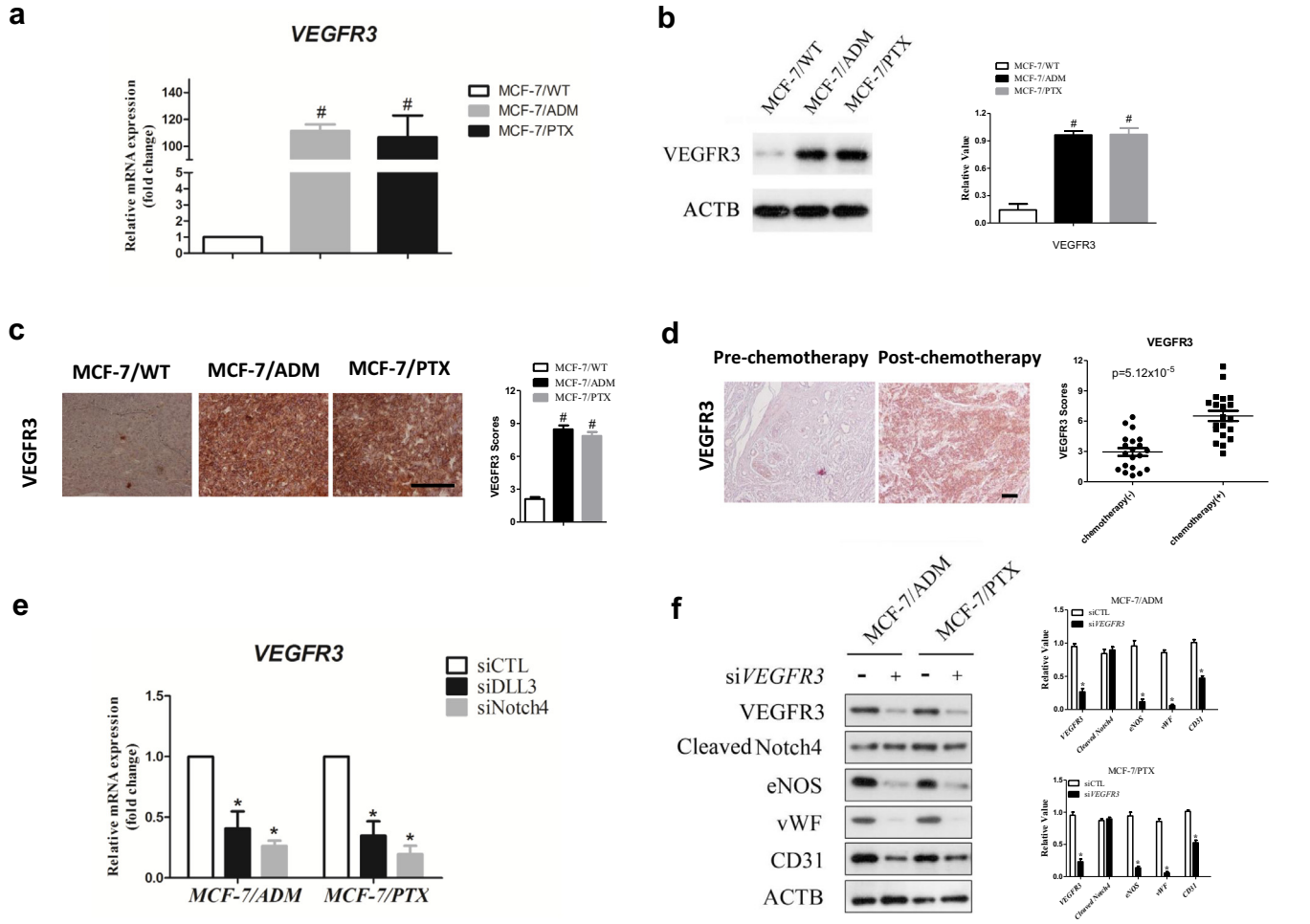

Fig. 8. Notch4 promotes formation of tumor-derived endothelial cells via VEGFR3 (a) Real-time reverse transcription-PCR and (b) Western blot for VEGFR3 in MCF-7/WT, MCF-7/ADM and MCF-7/PTX cells. (c) Representative images and summary data from immunohistochemical staining of VEGFR3 in paired pre- and post-chemotherapy breast cancer tissue from patients showing elevated VEGFR3 expression (n = 40). (d) Representative images and summary data from immunohistochemical staining of VEGFR3 in MCF-7/WT, MCF-7/ADM and MCF-7/PTX xenografts (e) Real-time reverse transcription-PCR for *VEGFR3* mRNA in MCF-7/ADM and MCF-7/PTX cells transfected with specific siRNA. (f) Western blot for VEGFR3, cleaved Notch4 and EC markers in MCF-7/ADM and MCF-7/PTX cells transfected with specific siRNA. Scale bars, 100 μm. Values are means ± SEM n = 3–4 #, $p < 0.05$, compared to MCF-7/WT *, $p < 0.05$, compared to MCF-7/ADM or MCF-7/PTX.

SNAI2 and HeyL were significantly decreased, which clearly suggests that the down-regulation of Notch4 or DLL3 expression results in the attenuated activity of Notch pathway (Fig. 7a). Subsequently, we assessed the effect of down-regulation of Notch4 and DLL3 on endothelial markers and the results showed that the expression of CD31, vWF, eNOS, CD105, and CD146 was strongly reversed in MCF-7/ADM and MCF-7/PTX cells transfected with Notch4 and DLL3 siRNAs (Fig. 7b and c). Silencing of Notch4 and DLL3 suppressed ability of tube formation in matrigel, low-density lipoprotein (LDL) uptake, NO release and VEGF secretion in MCF-7/ADM and MCF-7/PTX cells (Fig. 7d–f). Tumors with Notch4 and DLL3 siRNAs contained lower microvessel density and grew slower (Fig. 7g). Notch4 has been shown to regulate expression of VEGFR3 [34], and VEGFR3 played an important role of tumor angiogenesis [35,36]. We found that MCF-7/ADM and MCF-7/PTX cells had greater expression of VEGFR3 compared with MCF-7/WT cells (Fig. 8a and b). In addition, VEGFR3 expression was significantly up-regulated in clinical patients with chemotherapy, MCF-7/ADM xenografts and MCF-7/PTX xenografts (Fig. 8c and d). Silencing of Notch4 and DLL3 suppressed expression of VEGFR3 transcripts in MCF-7/ADM and MCF-7/PTX cells (Fig. 8e). Endothelial markers, CD31, vWF and eNOS were significantly decreased and cleaved Notch4 was not changed in MCF-7/ADM and MCF-7/PTX cells with silencing of VEGFR3 (Fig. 8f). These results clearly suggest that Notch pathway, especially DLL3 and Notch4 are important for tumor-derived endothelial cells under chemotherapy treatment.

4. Discussion

Although angiogenesis has become an important target in the treatment of breast cancer, anti-angiogenic agents have demonstrated limited activity and their underlying mechanism of action are still unknown. Here, we demonstrated that breast cancer cells in the context of chemotherapy are able to give rise to functional ECs in vascular networks mediated by Notch signaling in breast cancer.

It is generally known that breast cancer shows intratumoral heterogeneity. The ability of cancer stem-like cells to directly contribute to the tumor vasculature by EC differentiation has been reported previously in breast cancer, and similar endothelial potential is shared by ovarian cancer [37], glioblastoma and lymphoma [12–14]. Thus, it is believed CSC of these tumors contributed to this endothelial transition but the origin or stimuli of

CSCs remains unclear. CSCs may be derived from normal stem cells, their high-self renewal ability enables them to accumulate a series of genetic and epigenetic changes that promote them into CSCs. However, in this study, we may provide another explanation of CSCs origin: induced by chemotherapies, both clinical samples from neoadjuvant chemotherapy of breast cancer and in vitro/in vivo studies suggested the chemotherapy is able to induce normal tumor cells to give rise to endothelial cells through Notch pathways. Therefore, Our finding may explain the reason for failures in anti-angiogenesis therapy-combined neoadjuvant chemotherapy clinically: (1) Chemotherapy unveils the mesenchymal and CSCs features in tumor cells, thus enhance the tumor growth/metastasis by endowing anti-apoptosis ability to tumor cells from mesenchymal cells and CSCs; (2) chemotherapy promotes eNOS expression, VEGF secretion and NO release in those cancer cells, which is not only a feature of endothelial cells, but make tumor cells gaining of potent immunosuppressive capacity, a way of cancer cells to enter the blood circulation and metastasize to distant organ was offered; (3) chemotherapy enhanced the ability of cancer cells to organize into capillary-like structures by redifferentiation ability of mesenchymal cells and CSCs into endothelial, thus more nutrients and oxygen were provided to support tumor growth; (4) those mesenchyme or CSCs derived endothelial not only play an angiogenesis role, but also save the CSCs feature of hardly apoptosis when confront anti-angiogenic drugs.

Neoadjuvant chemotherapy, although widely applied worldwide to battle cancers, is a double blade sword. Without neoadjuvant chemotherapy, little discordance in estrogen receptor (ER), progesterone receptor (PR) and HER2 status has been reported; however, with neoadjuvant chemotherapy, discordance in ER, PR and HER2 from core needle biopsy and resected material is more evident, including a shift from luminal to basal-like partially by suppresses ER, PR and HER2 expression (triple negative) [38–43], the most lethal and aggressive subtype of breast cancer and closely associated with CSCs. In our study, we also found in the environment that mimic clinical chemotherapy, luminal type MCF-7 cells shifted to triple-negative MCF-7/ADM and MCF-7/PTX cells, thus in turn may facilitate them develop into CSCs. Thus, it cannot be excluded that dose intensity, cumulative dose of those widely used cytostatic chemotherapeutic agent might contribute to changes in ER, PR and HER2 status with the possible mechanisms: chemotherapy provides strong selection pressure, under which either tumor cell with survive advantage survives, or they develop survive advantages.

In conclusion, our findings may have considerable therapeutic implications. On the one hand, ECs bearing the same genomic alteration as cancer cells may show a different sensitivity to conventional anti-angiogenic treatments, such as VEGF/VEGFR targeting. On the other hand, our data raise the possibility of targeting the process of breast cancer give rise to ECs, thus offering new therapeutic options for cancer treatment.

Author contributions

XM, DXH and JJ conceived the project and designed the experiments with the help of PZ, LH and LH; XM, PZ, ZC, DXH performed the experiments with the help from QXP, FFD, XZ, YW, CLT; XM, PZ, ZC, DXH interpreted the data; XM, PZ, DXH, XQY and JJ wrote the manuscript.

Conflict of interest

No.

Acknowledgements

We thank Dr Teng Wang, LinFang Jin, XiaoWei Qi and Dong Hua in Affiliated hospital, Jiangnan University for collection of clinical samples and technical assistance, Prof Iain C Bruce for critical reading of the manuscript, and Prof Bo Jiang, Jing Xu, KeYu Lu in the State Key laboratory of Food Science and Technology, Jiangnan University for insightful comments and technical assistance. This work was supported by the China National Natural Science Foundation grants 91439131 and 81572940 (to XM), 31200126 and 31371317 (to DXH), 21305051 (to CLT); NSFC-RGC joint grant 81361168001 (to JJ); the National High-Technology Research and Development Program (863 Program) of China (2015AA020948 to XM); Natural Science Foundation for Distinguished Young Scholars of Jiangsu Province BK20140004 (to XM); the Program for New Century Excellent Talents in University of The Ministry of Education of China NCET-12-0880 (to XM); Fundamental Research Funds for the Central Universities JUSRP51311A and JUSRP51516 (to XM and JJ).

References

[1] J. Folkman, What is the evidence that tumors are angiogenesis dependent? J. Natl. Cancer Inst. 82 (1990) 4–6.
[2] J. Folkman, Angiogenesis in cancer, vascular, rheumatoid and other disease, Nat. Med. 1 (1995) 27–31.
[3] P. Carmeliet, R.K. Jain, Molecular mechanisms and clinical applications of angiogenesis, Nature 473 (2011) 298–307.
[4] N. Weidner, J.P. Semple, W.R. Welch, J. Folkman, Tumor angiogenesis and metastasis–correlation in invasive breast carcinoma, N. Engl. J. Med. 324 (1991) 1–8.
[5] D. Cameron, J. Brown, R. Dent, C. Jackisch, J. Mackey, X. Pivot, et al., Adjuvant bevacizumab-containing therapy in triple-negative breast cancer (BEATRICE): primary results of a randomised, phase 3 trial, Lancet Oncol. 14 (2013) 933–942.
[6] G. Bergers, D. Hanahan, Modes of resistance to anti-angiogenic therapy, Nat. Rev. Cancer 8 (2008) 592–603.
[7] F. Shojaei, N. Ferrara, Refractoriness to antivascular endothelial growth factor treatment: role of myeloid cells, Cancer Res. 68 (2008) 5501–5504.
[8] M. Pàez-Ribes, E. Allen, J. Hudock, T. Takeda, H. Okuyama, F. Viñals, et al., Antiangiogenic therapy elicits malignant progression of tumors to increased local invasion and distant metastasis, Cancer Cell 15 (2009) 220–231.
[9] E. Gunsilius, H.C. Duba, A.L. Petzer, C.M. Kähler, K. Grünewald, G. Stockhammer, et al., Evidence from a leukaemia model for maintenance of vascular endothelium by bone-marrow-derived endothelial cells, Lancet 355 (2000) 1688–1691.
[10] B. Streubel, A. Chott, D. Huber, M. Exner, U. Jäger, O. Wagner, et al., Lymphoma-specific genetic aberrations in microvascular endothelial cells in B-cell lymphomas, N. Engl. J. Med. 351 (2004) 250–259.
[11] G.M. Rigolin, C. Fraulini, M. Ciccone, E. Mauro, A.M. Bugli, C. De Angeli, et al., Neoplastic circulating endothelial cells in multiple myeloma with 13q14 deletion, Blood 107 (2006) 2531–2535.
[12] A. Pezzolo, F. Parodi, M.V. Corrias, R. Cinti, C. Gambini, V. Pistoia, Tumor origin of endothelial cells in human neuroblastoma, J. Clin. Oncol. 25 (2007) 376–383.
[13] L. Ricci-Vitiani, R. Pallini, M. Biffoni, M. Todaro, G. Invernici, T. Cenci, et al., Tumour vascularization via endothelial differentiation of glioblastoma stem-like cells, Nature 468 (2010) 824–828.
[14] R. Wang, K. Chadalavada, J. Wilshire, U. Kowalik, K.E. Hovinga, A. Geber, et al., Glioblastoma stem-like cells give rise to tumour endothelium, Nature 468 (2010) 829–833.
[15] Y. Soda, T. Marumoto, D. Friedmann-Morvinski, M. Soda, F. Liu, H. Michiue, et al., Transdifferentiation of glioblastoma cells into vascular endothelial cells, Proc. Natl. Acad. Sci. U.S.A. 108 (2011) 4274–4280.
[16] G. Dontu, W.M. Abdallah, J.M. Foley, K.W. Jackson, M.F. Clarke, M.J. Kawamura, Et al. In vitro propagation and transcriptional profiling of human mammary stem/progenitor cells, Genes Dev. 17 (2003) 1253–1270.
[17] G. Dontu, M.S. Wicha, Survival of mammary stem cells in suspension culture: implications for stem cell biology and neoplasia, J. Mammary Gland Biol. Neoplasia 10 (2005) 75–86.
[18] C. Grange, B. Bussolati, S. Bruno, V. Fonsato, A. Sapino, G. Camussi, Isolation and characterization of human breast tumor-derived endothelial cells, Oncol. Rep. 15 (2006) 381–386.
[19] B. Bussolati, C. Grange, A. Sapino, G. Camussi, Endothelial cell differentiation of human breast tumour stem/progenitor cells, J. Cell Mol. Med. 13 (2009) 309–319.
[20] R.J. Burcombe, A. Makris, P.I. Richman, F.M. Daley, S. Noble, M. Pittam, et al., Evaluation of ER, PgR, HER-2 and Ki-67 as predictors of response to

neoadjuvant anthracycline chemotherapy for operable breast cancer, Br. J. Cancer 92 (2005) 147–155.
[21] X. Ma, S. Qiu, J. Luo, Y. Ma, C.Y. Ngai, B. Shen, et al., Functional role of vanilloid transient receptor potential 4-canonical transient receptor potential 1 complex in flow-induced Ca^{2+} influx, Arterioscler. Thromb. Vasc. Biol. 30 (2010) 851–858.
[22] K. Al-Nedawi, B. Meehan, J. Micallef, V. Lhotak, L. May, A. Guha, et al., Intercellular transfer of the oncogenic receptor EGFRvIII by microvesicles derived from tumour cells, Nat. Cell Biol. 10 (2008) 619–624.
[23] M. Olivier, A. Langerød, P. Carrieri, J. Bergh, S. Klaar, J. Eyfjord, et al., The clinical value of somatic TP53 gene mutations in 1,794 patients with breast cancer, Clin. Cancer Res. 12 (2006) 1157–1167.
[24] M. Varna, G. Bousquet, L.F. Plassa, P. Bertheau, A. Janin, TP53 status and response to treatment in breast cancers, J. Biomed. Biotechnol. 2011 (2011) 284584.
[25] K. Agelopoulos, B. Greve, H. Schmidt, H. Pospisil, S. Kurtz, K. Bartkowiak, et al., Selective regain of egfr gene copies in CD44+/CD24−/low breast cancer cellular model MDA-MB-468, BMC Cancer 10 (2010) 78.
[26] N. Lv, X. Xie, Q. Ge, S. Lin, X. Wang, Y. Kong, et al., Epidermal growth factor receptor in breast carcinoma: association between gene copy number and mutations, Diagn. Pathol. 6 (2011) 118.
[27] M.M. Shao, F. Zhang, G. Meng, X.X. Wang, H. Xu, X.W. Yu, et al., Epidermal growth factor receptor gene amplification and protein overexpression in basal-like carcinoma of the breast, Histopathology 59 (2011) 264–273.
[28] D. Coradini, M. Fornili, F. Ambrogi, P. Boracchi, E. Biganzoli, TP53 mutation, epithelial-mesenchymal transition, and stemlike features in breast cancer subtypes, J. Biomed. Biotechnol. 2012 (2012) 254085.
[29] C. Kudo-Saito, H. Shirako, T. Takeuchi, Y. Kawakami, Cancer metastasis is accelerated through immunosuppression during Snail-induced EMT of cancer cells, Cancer Cell 15 (2009) 195–206.
[30] N.K. Kurrey, S.P. Jalgaonkar, A.V. Joglekar, A.D. Ghanate, P.D. Chaskar, R.Y. Doiphode, et al., Snail and slug mediate radioresistance and chemoresistance by antagonizing p53-mediated apoptosis and acquiring a stem-like phenotype in ovarian cancer cells, Stem Cells 27 (2009) 2059–2068.
[31] Z. Wang, Y. Li, D. Kong, S. Banerjee, A. Ahmad, A.S. Azmi, S. Ali, et al., Acquisition of epithelial–mesenchymal transition phenotype of gemcitabine-resistant pancreatic cancer cells is linked with activation of the notch signaling pathway, Cancer Res. 69 (2009) 2400–2407.
[32] C.E.S. Min, D.H. Sherr, G.E. Sonenshein, NF-nB and epithelial to mesenchymal transition of cancer, J. Cell. Biochem. 104 (2008) 733–744.
[33] U.S.J. Wellner, U.C. Burk, O. Schmalhofer, F. Zhu, A. Sonntag, B. Waldvogel, et al., The EMT-activator ZEB1 promotes tumorigenicity by repressing stemness-inhibiting microRNAs, Nat. Cell Biol. 11 (2009) 1487–1495.
[34] C.J. Shawber, Y. Funahashi, E. Francisco, M. Vorontchikhina, Y. Kitamura, S.A. Stowell, et al., Notch alters VEGF responsiveness in human and murine endothelial cells by direct regulation of VEGFR-3 expression, J. Clin. Invest. 117 (2007) 3369–3382.
[35] R. Valtola, P. Salven, P. Heikkilä, J. Taipale, H. Joensuu, M. Rehn, et al., VEGFR-3 and its ligand VEGF-C are associated with angiogenesis in breast cancer, Am. J. Pathol. 154 (1999) 1381–1390.
[36] A.N. Witmer, B.C. van Blijswijk, J. Dai, P. Hofman, T.A. Partanen, G.F. Vrensen, et al., VEGFR-3 in adult angiogenesis, J. Pathol. 195 (2001) 490–497.
[37] A.B. Alvero, R. Chen, H.H. Fu, M. Montagna, P.E. Schwartz, T. Rutherford, et al., Molecular phenotyping of human ovarian cancer stem cells unravels the mechanisms for repair and chemoresistance, Cell Cycle 8 (2009) 158–166.
[38] R.J. Burcombe, A. Makris, P.I. Richman, F.M. Daley, S. Noble, M. Pittam, et al., Evaluation of ER, PgR, HER-2 and Ki-67 as predictors of response to neoadjuvant anthracycline chemotherapy for operable breast cancer, Br. J. Cancer 92 (2005) 147–155.
[39] M. Arnedos, A. Nerurkar, P. Osin, R. A'Hern, I.E. Smith, M. Dowsett, Discordance between core needle biopsy (CNB) and excisional biopsy (EB) for estrogen receptor (ER), progesterone receptor (PgR) and HER2 status in early breast cancer (EBC), Ann. Oncol. 20 (2009) 1948–1952.
[40] H. Neubauer, C. Gall, U. Vogel, R. Hornung, D. Wallwiener, E. Solomayer, et al., Changes in tumour biological markers during primary systemic chemotherapy (PST), Anticancer Res. 28 (2008) 1797–1804.
[41] T. Hirata, C. Shimizu, K. Yonemori, A. Hirakawa, T. Kouno, K. Tamura, et al., Change in the hormone receptor status following administration of neoadjuvant chemotherapy and its impact on the long-term outcome in patients with primary breast cancer, Br. J. Cancer 101 (2009) 1529–1536.
[42] O. Tacca, F. Penault-Llorca, C. Abrial, M.A. Mouret-Reynier, I. Raoelfils, X. Durando, et al., Changes in and prognostic value of hormone receptor status in a series of operable breast cancer patients treated with neoadjuvant chemotherapy, Oncologist 12 (2007) 636–643.
[43] S. Van de Ven, V.T. Smit, T.J. Dekker, J.W. Nortier, J.R. Kroep, Discordances in ER, PR and HER2 receptors after neoadjuvant chemotherapy in breast cancer, Cancer Treat. Rev. 37 (2011) 422–430.